

A PARALLEL PROCESSING APPROACH TO FILTERBANK MULTICARRIER MIMO TRANSMISSION UNDER STRONG FREQUENCY SELECTIVITY

Xavier Mestre, David Gregoratti

Centre Tecnològic de Telecomunicacions de Catalunya, Castelldefels, Barcelona (Spain)

ABSTRACT

The problem of MIMO transmission using filterbank multicarrier (FBMC) modulations in strong frequency selective channels is considered. A novel architecture for the implementation of MIMO precoders and linear receivers is derived, which consists of multiple parallel stages that are combined at the per-subcarrier level. Each of these stages is constructed like a classical FBMC modulator/demodulator, using the successive derivatives of the prototype pulse instead of the original one. The performance of the proposed architecture is theoretically characterized in terms of the residual distortion power at the output of the receiver, assuming an asymptotically large number of subcarriers. Results demonstrate the effectiveness of the proposed architecture in MIMO channels with severe frequency selectivity.

Index Terms— Filterbank Multicarrier, MIMO, FBMC/OQAM, spatial multiplexing.

1. INTRODUCTION AND SIGNAL MODEL

Filterbank multicarrier modulations (FBMC) are currently being considered as good alternatives to classical cyclic-prefix OFDM (CP-OFDM) for the physical layer of future 5G mobile communication standards. The main advantage of FBMC over CP-OFDM is twofold: the lack of cyclic prefix, which increases the spectral efficiency, and the use of non-rectangular pulse shaping, which improves the spectral localization and reduces the need for guard bands. Under relatively mild channel frequency selectivity, the channel response can be assumed to be approximately flat within each subcarrier band, which allows the use of single-tap per-subcarrier equalizers as in CP-OFDM. However, in the presence of strong channel frequency selectivity, the channel can no longer be approximately flat within each subcarrier band, and FBMC modulations require more sophisticated equalization systems (see e.g. [1] and references therein). In practical terms, if the receiver keeps using a single-tap per-subcarrier equalizer in the presence of a highly frequency selective channel, its output will appear contaminated by a residual distortion superposed to the background noise.

The effect of this residual distortion is much more devastating in MIMO transmissions, basically due to a superposition effect of the multiple parallel antennas/streams [2, 3, 4]. This incremental distortion effect in MIMO contexts has traditionally been mitigated using complex receiver strategies, such as sophisticated equalization architectures [5, 6, 7], or algorithms based on successive interference cancellation [8, 9, 7]. More recent approaches have additionally considered the optimization of the transmitter architecture in order to

This work was partially supported by the Catalan and Spanish Government under grants 2009SGR1046 and TEC2011-29006-C03-01, and by the European Commission under the Emphatic project ICT-318362.

mitigate the effect of the channel frequency selectivity. For example, [10] considers the optimization of the precoder/linear receiver pair in order to achieve spatial diversity while minimizing the residual distortion at the output of the receiver. A related approach can be found in [11, 12], where a polynomial-based (multi-tap) SVD precoder is applied together with an equivalent multi-tap equalizer at the receiver.

Here we take an approach similar to the one in [13] and propose a general architecture that can be used to implement multiple MIMO transceivers (precoder plus linear receiver) in highly frequency selective channels. Our approach is substantially different from the one in [10, 11, 12], because rather than focusing on a particular objective to optimize the transceiver, the proposed architecture provides a general framework that can be used to construct a variety of MIMO transceivers.

More specifically, let us consider a linear MIMO transceiver with N_T transmit and N_R receive antennas. Let $\mathbf{H}(\omega)$ denote an $N_R \times N_T$ matrix containing the frequency response of the MIMO channel, so that the (i, j) th entry of $\mathbf{H}(\omega)$ contains the frequency response between the j th transmit and the i th receive antennas. We assume that the MIMO system is used for the transmission of N_S parallel streams, $1 \leq N_S \leq \min\{N_R, N_T\}$, which are FBMC modulated signals with $2M$ subcarriers. To simplify the exposition, we will consider exponentially modulated, uniform and maximally decimated FBMC signals based on OQAM (FBMC/OQAM) [14], although our approach can be generalized to other types of FBMC signals. We will denote by $\mathbf{s}(\omega)$ an $N_S \times 1$ column vector that contains the frequency response of the signal transmitted at each of the N_S parallel streams.

Assume that the transmitter applies a frequency-dependent linear precoder, which will be denoted by the $N_T \times N_S$ matrix $\mathbf{A}(\omega)$. Let $\mathbf{y}(\omega)$ denote an $N_R \times 1$ column vector containing the frequency response of the received signals in noise, namely

$$\mathbf{y}(\omega) = \mathbf{H}(\omega)\mathbf{A}(\omega)\mathbf{s}(\omega) + \mathbf{n}(\omega)$$

where $\mathbf{n}(\omega)$ is the additive Gaussian white noise. We assume that the receiver estimates the transmitted symbols by linearly transforming the received signal vector $\mathbf{y}(\omega)$ through a certain frequency-dependent $N_R \times N_S$ receive matrix $\mathbf{B}(\omega)$, namely

$$\hat{\mathbf{s}}(\omega) = \mathbf{B}^H(\omega)\mathbf{y}(\omega).$$

The whole ideal frequency-selective transceiver chain can be implemented as shown in Figure 1, where we have denoted by $p[n]$ and $q[n]$ the real-valued prototype pulses used at the transmitter and at the receiver respectively (we assume that they may be generally different).

The main problem with the MIMO architecture presented in Figure 1 comes from the fact that, in practice, the frequency-dependent matrices $\mathbf{A}(\omega)$, $\mathbf{B}(\omega)$ need to be implemented using real filters.

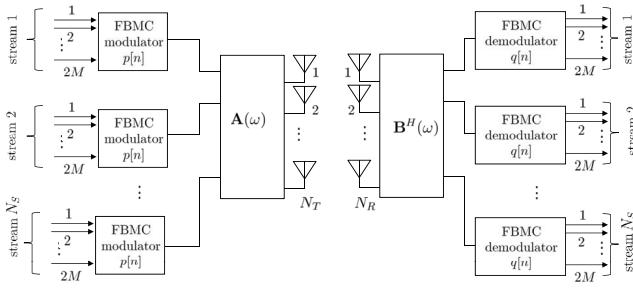


Fig. 1. Ideal implementation of a frequency selective precoder $\mathbf{A}(\omega)$ and a linear receiver $\mathbf{B}^H(\omega)$ in a FBMC modulation system with $2M$ carriers.

These filters may not have finite impulse response and, even when this is the case, they might be difficult to implement due to the number of coefficients that may be involved. This can be partly solved in multicarrier modulations, assuming that the channel frequency selectivity is not severe and therefore the channel is approximately flat at each subcarrier frequency band. When this is the case, one can construct the MIMO precoder/receiver operations by applying the matrices $\mathbf{A}(\omega_k)$, $\mathbf{B}(\omega_k)$ to each subcarrier stream, where here ω_k denotes the central frequency associated with the k th subcarrier (i.e. $\omega_k = \pi(k-1)/M$). This is further illustrated in Figure 2 for the particular case of $N_T = 2$ antennas in a FBMC multi-antenna transmitter (a similar implementation would hold for the receive side, replacing $\mathbf{A}(\omega_k)$ by the corresponding $\mathbf{B}(\omega_k)$).

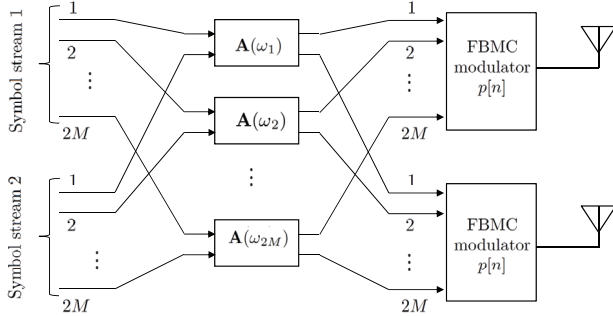


Fig. 2. Traditional implementation of the frequency-selective precoder in multicarrier modulations, for the specific case of N_T transmit antennas and $2M$ subcarriers.

As pointed out above, this solution is only effective when the channel frequency selectivity is mild enough to guarantee that each sub-carrier observes a frequency non-selective channel. However this is hardly the case in practical wireless systems, which will suffer from a non-negligible distortion at the output of the receiver that will severely impair the performance of the MIMO transmission. Next, we propose an alternative solution that tries to minimize this effect.

2. PROPOSED APPROACH

In this subsection we propose an alternative solution that, with some additional complexity, significantly mitigates the distortion caused by the channel frequency selectivity. Assume that $P(\exp j\omega)$ and $Q(\exp j\omega)$ contain –up to a constant factor– the frequency response

of the transmit and receive prototype pulses $p[n]$ and $q[n]$, respectively. Let us consider the combination of the FBMC transmission with the frequency selective MIMO precoder $\mathbf{A}(\omega)$. More specifically, consider the k th subcarrier associated with the n_S th MIMO signal stream that is sent through the n_T th transmit antenna. Assuming that the ideal frequency-selective precoder matrix $\mathbf{A}(\omega)$ is implemented, this stream will effectively go through a transmit filter with equivalent frequency response:

$$P(\exp j(\omega - \omega_k)) \{\mathbf{A}(\omega)\}_{n_T, n_S}.$$

Now, assume that the precoding matrix $\mathbf{A}(\omega)$ is an analytic function in the frequency domain, so that we can express it as its Taylor series around ω_k , namely

$$\mathbf{A}(\omega) = \sum_{\ell=0}^{\infty} \frac{1}{\ell!} \mathbf{A}^{(\ell)}(\omega_k) (\omega - \omega_k)^{\ell} \quad (1)$$

where $\mathbf{A}^{(\ell)}(\omega_k)$ denotes the ℓ th derivative of $\mathbf{A}(\omega)$ evaluated at $\omega = \omega_k$. Using this Taylor series expression, we can describe the frequency response of the ideal transmit chain as

$$\sum_{\ell=0}^{\infty} \frac{1}{\ell!} P(\exp j(\omega - \omega_k)) \{\mathbf{A}^{(\ell)}(\omega_k)\}_{n_T, n_S} (\omega - \omega_k)^{\ell}.$$

The idea behind the classical precoder implementation in Figure 2 is to truncate this Taylor series development and to consider only its first term. When this is the case, the transmitter frequency response that is effectively implemented takes the form $P(\exp j(\omega - \omega_k)) \{\mathbf{A}(\omega_k)\}_{n_T, n_S}$, which corresponds to a single weight multiplication of each subcarrier signal, as shown in Figure 2.

Here, we suggest to go a bit further and consider the truncation of the above series representation to include its first K_T terms, so that the transmitter filter has an effective frequency response equal to

$$\sum_{\ell=0}^{K_T-1} \frac{1}{\ell!} P(\exp j(\omega - \omega_k)) (\omega - \omega_k)^{\ell} \{\mathbf{A}^{(\ell)}(\omega_k)\}_{n_T, n_S}. \quad (2)$$

The main advantage of extending this truncation to the case $K_T > 1$ comes from the fact that one can effectively implement the above filter by using K_T parallel FBMC modulators, together with K_T parallel precoders based on single-tap per-subcarrier implementations. To see this, observe that if the prototype pulse $p[n]$ is a sampled version of an original waveform $p(t)$ (with some abuse of notation) one can actually see $P(\exp j(\omega - \omega_k)) (2Mj)^{\ell} (\omega - \omega_k)^{\ell}$ as the frequency response of the sampled waveform corresponding to the ℓ th derivative of $p(t)$. Hence, when ω is relatively close to ω_k , the frequency response in (2) can be equivalently formulated as

$$\sum_{\ell=0}^{K_T-1} \frac{1}{\ell!} \left(\frac{-j}{2M} \right)^{\ell} P^{(\ell)}(\exp j(\omega - \omega_k)) \{\mathbf{A}^{(\ell)}(\omega_k)\}_{n_T, n_S}$$

where $P^{(\ell)}(\exp j\omega)$ is –up to a constant factor– the frequency response associated with the ℓ th pulse derivative. Now, observe that each term of the above sum has exactly the same form as the transmitter in Figure 2, replacing the actual precoder matrix $\mathbf{A}(\omega_k)$ and the original prototype pulse $P(\exp j\omega)$ by their successive derivatives $\mathbf{A}^{(\ell)}(\omega_k)$, $P^{(\ell)}(\exp j\omega)$. Therefore, the K_T -term truncation of the ideal transmit precoder frequency response can be implemented

by combining a set of K_T parallel precoders as shown in Figure 3, where we represent the proposed implementation of the transmit precoder when the number of parallel stages was fixed to $K_T = 2$ and the number of transmit antennas to $N_T = 2$. We have represented in red dotted line the additional stage that needs to be superposed to the original one (in black solid line), which is the same as in Figure 2. Obviously, we can follow the same approach in order to approximate the ideal frequency selective linear receiver matrix $\mathbf{B}(\omega)$ in combination with the receive prototype pulse $Q(\exp j(\omega - \omega_k))$.

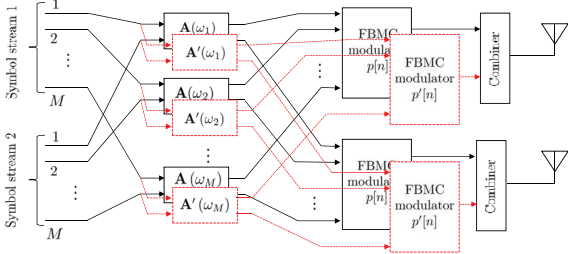


Fig. 3. Proposed implementation of the frequency-selective precoder for the specific case of $N_T = 2$ transmit antennas and $N_T = 2$ parallel stages.

3. PERFORMANCE ASSESSMENT

From all the above, we can conclude that we can approximate the ideal frequency-selective precoder/linear receiver as depicted in Figure 1 by simply increasing the number of parallel stages (K_T, K_R) that are implemented at the transmitter and at the receiver. In this subsection, we investigate the residual distortion effect of this implementation at the output of the receiver, which will be the determining factor in order to fix these two parameters so as to reach a certain performance quality. To that effect, we will make some very simple assumptions that will considerably simplify the analysis:

(As1) The transmit and receive prototype pulses $p[n], q[n]$ are of length $2M\kappa$, where κ is an integer that is typically referred to as the overlapping factor. Furthermore, these pulses are obtained by discretization of smooth analog waveforms $p(t), q(t)$, so that

$$p[n] = p\left(\left(n - \frac{2M\kappa + 1}{2}\right) \frac{T_s}{2M}\right), \quad n = 1, \dots, 2M\kappa$$

and equivalently for $q[n]$, where T_s is the sampling period. Furthermore, the pulses $p(t), q(t)$ are either symmetric or anti-symmetric in the time domain and their successive derivatives are null at the end-points of their support, namely at $t = \pm T_s \kappa / 2$.

(As2) The complex symbols are drawn from a bounded constellation, and their real and imaginary parts are independent, identically distributed random variables with zero mean and power $P_s/2$.

(As3) All frequency-dependent quantities ($\mathbf{A}(\omega), \mathbf{B}(\omega), \mathbf{H}(\omega)$) are smooth functions of ω .

Under these assumptions, it is possible to characterize the behavior of the residual distortion at the output of the receiver, assuming that the number of subcarriers is asymptotically high ($M \rightarrow \infty$). To describe the residual distortion power that is observed at the output of the receiver, it is convenient to define some pulse-specific quantities as follows. Consider two general pulses $p[n], q[n]$ of length $2M\kappa$, and let \mathbf{P} and \mathbf{Q} denote two $2M \times \kappa$ matrices obtained by

arranging the original samples in columns. In other words, the k th row of \mathbf{P} (resp. \mathbf{Q}) contains the k th polyphase component of the original pulse $p[n]$ (resp. $q[n]$). Next, consider two $2M \times (2\kappa - 1)$ matrices $\mathcal{R}(p, q)$ and $\mathcal{S}(p, q)$ obtained as

$$\begin{aligned} \mathcal{R}(p, q) &= \mathbf{P} \circledast \mathbf{J}_{2M} \mathbf{Q} \\ \mathcal{S}(p, q) &= (\mathbf{J}_2 \otimes \mathbf{I}_M) \mathbf{P} \circledast \mathbf{J}_{2M} \mathbf{Q} \end{aligned}$$

where \circledast indicates row-wise convolution between matrices, \mathbf{J}_{2M} is the anti-identity matrix of size $2M$, and \otimes denotes Kronecker product. Given four different pulses of length $2M\kappa$, i.e. $p_1[n], q_1[n], p_2[n], q_2[n]$, we define

$$\eta_{(p_1, q_1, p_2, q_2)}^{(+,-)} = \frac{1}{2M} \text{tr} \left[\mathcal{R}(p_1, q_1) \mathcal{R}^T(p_2, q_2) \mathbf{U}^+ + \mathcal{S}(p_1, q_1) \mathcal{S}^T(p_2, q_2) \mathbf{U}^- \right]$$

where $\mathbf{U}^+ = \mathbf{I}_2 \otimes (\mathbf{I}_M + \mathbf{J}_M)$ and $\mathbf{U}^- = \mathbf{I}_2 \otimes (\mathbf{I}_M - \mathbf{J}_M)$. The quantity $\eta_{(-,+)}^{(-,+)}$ is equivalently defined, but swapping \mathbf{U}^+ and \mathbf{U}^- .

Let us consider the proposed multi-stage frequency-selective architecture with K_T parallel stages at the transmitter and K_R parallel stages at the receiver. This means that the Taylor series of $\mathbf{A}(\omega)$ in (1) is truncated to the first K_T terms, whereas the Taylor series of $\mathbf{B}(\omega)$ is truncated to the first K_R terms. If all the terms of order higher than K_T in the Taylor series representation of $\mathbf{A}(\omega)$ are zero¹, we redefine $K_T = \infty$. We proceed equivalently for $\mathbf{B}(\omega)$ and K_R . With these definitions, we take $K = \min\{K_T, K_R\}$ and denote by $p_N^{(K)}$ and $\mathbf{A}^{(K)}(\omega)$ (resp. $q_N^{(K)}$ and $\mathbf{B}^{(K)}(\omega)$) the sampled version of the K th derivative of $p(t)$ and the K th derivative of $\mathbf{A}(\omega)$ (resp. $q(t)$ and $\mathbf{B}(\omega)$). The proof of the following result can be obtain along the lines of [13] (details are omitted due to space constraints).

Theorem 1 Under assumptions (As1-As3), as $M \rightarrow \infty$, the residual distortion power observed at the k th subcarrier associated with the n th symbol stream takes the form

$$\begin{aligned} P_e(k, n) &= \sum_{n_S=1}^{N_S} \left| A_{n,n_S}^{(K)}(k) \right|^2 \eta_{(p_N^{(K)}, q_N^{(K)}, p_N^{(K)}, q_N^{(K)})}^{(+,-)} \\ &+ 2 \sum_{n_S=1}^{N_S} \Re \left[A_{n,n_S}^{(K)}(k) \right] \Re \left[B_{n,n_S}^{(K)}(k) \right] \eta_{(p_N^{(K)}, q_N^{(K)}, p_N^{(K)}, q_N^{(K)})}^{(+,-)} \\ &+ 2 \sum_{n_S=1}^{N_S} \Im \left[A_{n,n_S}^{(K)}(k) \right] \Im \left[B_{n,n_S}^{(K)}(k) \right] \eta_{(p_N^{(K)}, q_N^{(K)}, p_N^{(K)}, q_N^{(K)})}^{(-,+)} \\ &+ \sum_{n_S=1}^{N_S} \left| B_{n,n_S}^{(K)}(k) \right|^2 \eta_{(p_N^{(K)}, q_N^{(K)}, p_N^{(K)}, q_N^{(K)})}^{(-,+)} + O\left(\frac{1}{(2M)^{2(K+1)}}\right) \end{aligned}$$

where $\Re[\cdot]$ and $\Im[\cdot]$ represent the real and imaginary part and where

$$A_{n,n_S}^{(K)}(k) = \frac{\sqrt{2}(-j)^K}{K!(2M)^K} \left\{ \mathbf{B}^H(\omega_k) \mathbf{H}(\omega_k) \mathbf{A}^{(K)}(\omega_k) \right\}_{n,n_S}$$

$$B_{n,n_S}^{(K)}(k) = \frac{\sqrt{2}(-j)^K}{K!(2M)^K} \left\{ \mathbf{B}^{(K)}(\omega_k)^H \mathbf{H}(\omega_k) \mathbf{A}(\omega_k) \right\}_{n,n_S}$$

with $\mathbf{A}^{(K)}(\omega)$ and $\mathbf{B}^{(K)}(\omega)$ denoting the K th order derivatives of $\mathbf{A}(\omega)$ and $\mathbf{B}(\omega)$ respectively.

¹This would be the case if $\mathbf{A}(\omega)$ does not depend on ω , or more generally when $\mathbf{A}(\omega)$ is a polynomial matrix of degree lower than K_T .

It is worth noting that the performance of the proposed system is always dictated by the minimum between K_T and K_R , so clearly no additional advantage is obtained when more parallel stages are implemented at either side of the communication link. On the other hand, it is also interesting to observe that the residual distortion increases linearly with the number of parallel streams that are transmitted, which explains why FBMC modulations are so sensitive to distortion in the MIMO spatial multiplexing setting.

4. PERFORMANCE ANALYSIS

In this section, we illustrate the performance of the proposed MIMO transceiver architecture and compare it with the theoretical description provided in Theorem 1. We considered a system with 512 subcarriers and an intercarrier separation of 15kHz. The prototype pulse was fixed to be the same at both transmitter and receiver, and it was designed to have an overlapping factor equal to $\kappa = 2$ and perfect reconstruction properties [14].

The number of antennas was fixed to 2 at both the transmitter and the receiver, namely $N_T = N_R = 2$, and the four resulting MIMO channels were simulated as independent and fixed random realizations of an ITU Extended Vehicular A (EVA) channel model [15]. Figure 4 represents the frequency response of the two eigenvalues of the corresponding MIMO channel matrix used in the simulations. Let $\mathbf{H}(\omega) = \mathbf{U}(\omega)\Lambda(\omega)\mathbf{V}^H(\omega)$ denote the SVD of the channel matrix $\mathbf{H}(\omega)$, so that $\mathbf{U}(\omega)$ and $\mathbf{V}(\omega)$ are two orthonormal matrices that contain the left and right singular vectors of $\mathbf{H}(\omega)$, and where $\Lambda(\omega)$ is a diagonal matrix that contains the associated singular values. In these simulations, the precoder was taken as $\mathbf{A}(\omega) = \mathbf{V}(\omega)$ (maximum capacity precoding under Gaussian signalling) whereas the linear receiver performed an inversion of the resulting channel, namely $\mathbf{B}(\omega) = \mathbf{U}(\omega)\Lambda^{-1}(\omega)$.

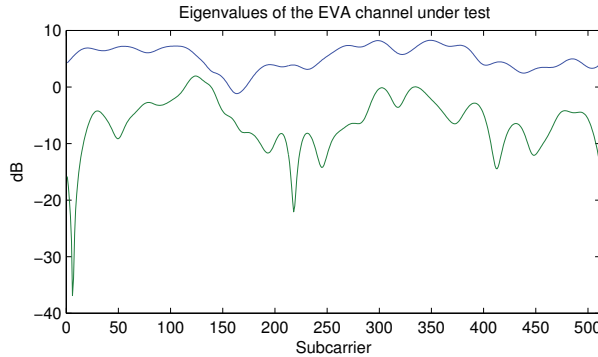


Fig. 4. Eigenvalues of the simulated MIMO channel.

In order to validate the expressions for the residual distortion, we considered a noiseless scenario where we simulated a set of 1000 multicarrier symbols (drawn from a QPSK modulation) and measured the signal to distortion power ratio at the output of the receiver. Results for the two transmitted streams are represented in Figure 5 for different configurations in the number of parallel stages at the transmit (K_T) and receive (K_R) sides, where solid lines represent the theoretical performance as described by Theorem 1 whereas markers are numerical performance values. Observe that there is a perfect match between them, and the simulated results are virtually indistinguishable from the theoretical ones.

As for the actual behavior of the transceiver, it must be first pointed out that the performance that can be achieved with the tra-

ditional MIMO architecture (which corresponds to the case $K_R = K_T = 1$) is quite limited, and that important gains can be achieved by using the proposed MIMO architecture with multiple parallel stages at both sides of the communications link. On the other hand, simulations confirm that –in general terms– performance is roughly dictated by the minimum number of parallel stages used at the transmit and receive sides, that is the minimum between K_R and K_T . This can be clearly seen in the upper plot of Figure 5 (strongest eigenmode), were it is clearly observed that no clear advantage is obtain unless two parallel stages are implemented at both transmitter and receiver.

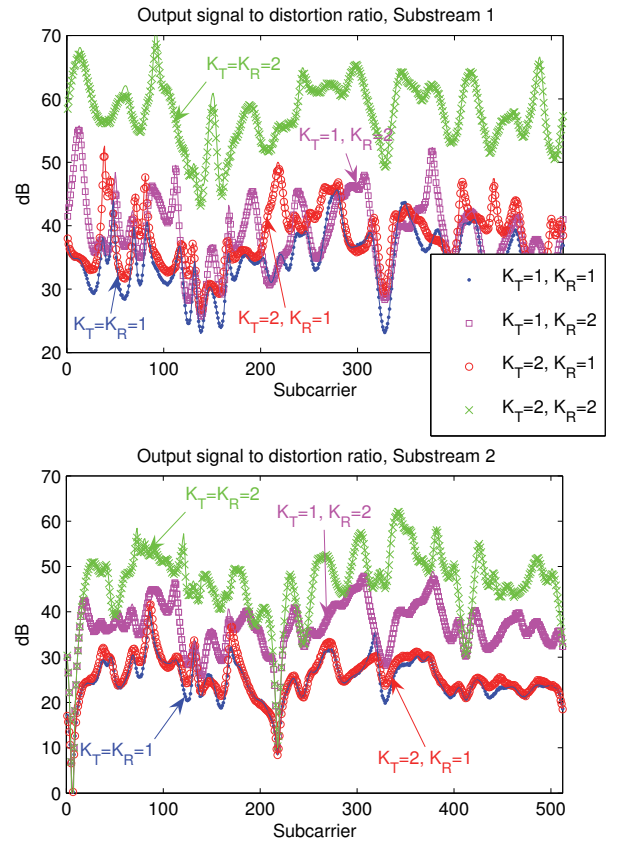


Fig. 5. Signal to distortion power ratio measured at the output of the receiver when the transmitter uses SVD-type precoding and the receiver performs channel inversion.

5. CONCLUSIONS

A novel MIMO architecture for FBMC modulations under channels with severe frequency selectivity has been proposed. This architecture can be applied to any MIMO transceiver consisting of a frequency-dependent precoder and a frequency-dependent linear receiver. The performance of the proposed approach has been characterized in the asymptotic regime when the number of subcarriers increases to infinity, and simulation results indicate that these asymptotic expressions are very good approximations of the non-asymptotic reality. Finally, it has been shown that the proposed architecture provides a significant advantage in terms of reduced residual distortion at the output of the receiver.

6. REFERENCES

- [1] T. Ihalainen, T. H. Stitz, M. Rinne, and M. Renfors, "Channel equalization in filter bank based multicarrier modulation for wireless communications," *EURASIP Journal on Advances in Signal Processing*, vol. 2007, pp. 1–18, 2007.
- [2] I. Estella, A. Pascual-Iserte, and M. Payaró, "OFDM and FBMC performance comparison for multistream MIMO systems," in *Proceedings of the Future Network and MobileSummit*, (Florence, Italy), June 2010.
- [3] M. Nájar, M. Payaró, E. Kofidis, M. Tanda, J. Louveaux, M. Renfors, T. Hidalgo, D. L. Ruyet, C. Lélé, R. Zacaria, and M. Bellanger, "MIMO techniques and beamforming," Deliverable D4.2, ICT PHYDYAS project, PHYSical layer for DYnamic AccesS and cognitive radio, Feb. 2010.
- [4] M. Payaró, A. Pascual-Iserte, and M. Nájar, "Performance comparison between FBMC and OFDM in MIMO systems under channel uncertainty," in *Proceedings of the European Wireless Conference (EW)*, (Lucca), pp. 1023 – 1030, April 2010.
- [5] E. Kofidis and A. Rontogiannis, "Adaptive BLAST decision-feedback equalizer for MIMO-FBMC/OQAM systems," in *Proceedings of the IEEE 21st International Symposium on Personal Indoor and Mobile Radio Communications, PIRMC*, (Istanbul, Turkey), pp. 841 – 846, Sept. 2010.
- [6] T. Ihalainen, A. Ikhlef, J. Louveaux, and M. Renfors, "Channel equalization for multi-antenna FBMC/OQAM receivers," *IEEE Trans. on Vehicular Technology*, vol. 60, pp. 2070–2085, Jun. 2011.
- [7] M. Nájar, C. Bader, F. Rubio, E. Kofidis, M. Tanda, J. Louveaux, M. Renfors, and D. L. Ruyet, "Mimo channel matrix estimation and tracking," Deliverable D4.1, ICT PHYDYAS project, PHYSical layer for DYnamic AccesS and cognitive radio, Jan. 2009.
- [8] A. Ikhlef and J. Louveaux, "Per-subchannel equalization for MIMO FBMC/OQAM systems," in *Proc. of the IEEE Pacific Rim Conference on Communications, Computers and Signal Processing*, (Victoria, Canada), p. 559–564., Aug 2009.
- [9] M. E. Tabach, J. Javaudin, and M. Hélard, "Spatial data multiplexing over OFDM/OQAM modulations," in *Proceedings of the IEEE International Conference on Communications*, (Glasgow, Scotland), pp. 4201 – 4206, June 2007.
- [10] M. Caus and A. Pérez-Neira, "Transmitter-receiver designs for highly frequency selective channels in MIMO FBMC systems," *IEEE Transactions on Signal Processing*, vol. 60, pp. 6519–6532, Dec. 2012.
- [11] N. Moret, A. Tonello, and S. Weiss, "MIMO precoding for filter bank modulation systems based on PSVD," in *Proceedings of the IEEE Vehicular Technology Conference (VTC Spring)*, (Yokohama, Japan), May 2011.
- [12] S. Weiss, N. Moret, A. Millar, A. Tonello, and R. Stewart, "Initial results on an MMSE precoding and equalisation approach to MIMO PLC channels," in *Proceedings of the IEEE International Symposium on Power Line Communications and Its Applications ISPLC*, (Udine, Italy), pp. 146 – 152, Apr. 2011.
- [13] X. Mestre, M. Majoral, and S. Pfletschinger, "An asymptotic approach to parallel equalization of filter bank multicarrier signals," *IEEE Trans. on Sig. Proc.*, vol. 61, pp. 3592–3606, July 2013.
- [14] P. Siohan, C. Siclet, and N. Lacaille, "Analysis and design of OFDM/OQAM systems based on filterbank theory," *IEEE Trans. on Sig. Proc.*, vol. 50, pp. 1170–1183, May 2002.
- [15] G. T. 36.101, "User equipment (UE) radio transmission and reception," tech. rep., 3rd Generation Partnership Project; Technical Specification Group Radio Access Network; E-UTRA, <http://www.3gpp.org>, 2013.